Role of the Transition Metal in Metallaborane Chemistry. Reactivity of $(Cp^*ReH_2)_2B_4H_4$ with BH_3·thf, CO, and $Co_2(CO)_8$

Sundargopal Ghosh, Xinjian Lei, Maoyu Shang, and Thomas P. Fehlner*

Department of Chemistry and Biochemistry, University of Notre Dame, Notre Dame, Indiana 46556-5670

Received June 6, 2000

The reaction of Cp^*ReCl_4, $[Cp^*ReCl_3]_2$, or $[Cp^*ReCl_2]_2$ ($Cp^* = \eta^5$-C_5Me_5) with $LiBH_4$ leads to the formation of 7-skeletal-electron-pair (7-sep) $(Cp^*ReH_2)_2(B_2H_3)_2$ (**1**) together with Cp^*ReH_6. Compound **1** is metastable and eliminates H_2 at room temperature to generate 6-sep $(Cp^*ReH_2)_2B_4H_4$ (**2**). The reaction of **2** with BH_3·thf produces 7-sep $(Cp^*Re)_2B_7H_7$, a hypoelectronic cluster characterized previously. Heating of **2** with 1 atm of CO leads to 6-sep $(Cp^*ReCO)(Cp^*ReH_2)B_4H_4$ (**3**). Both **2** and **3** have the same bicapped Re_2B_2 tetrahedral cluster core structure. Monitoring the reaction of **2** with CO at room temperature by NMR reveals the formation of a 7-sep, metastable intermediate, $(Cp^*ReCO)(Cp^*ReH_2)(B_2H_3)_2$ (**4**), which converts to **3** on heating. An X-ray structure determination reveals two isomeric forms (**4**-*cis* and **4**-*trans*) in the crystallographic asymmetric unit which differ in geometry relative to the disposition of the metal ancillary ligands with respect to the Re−Re bond. The presence of these isomers in solution is corroborated by the solution NMR data and the infrared spectrum. In both isomers, the metallaborane core consists of fused B_2Re_2 tetrahedra sharing the Re_2 fragment. On the basis of similarities in electron count and spectroscopic data, **1** also possesses the same bitetrahedral structure. The reaction of **2** with $Co_2(CO)_8$ results in the formal replacement of the four rhenium hydrides with a 4-electron $Co_2(CO)_5$ fragment, thereby closing the open face in **2** to produce the 6-sep hypoelectronic cluster $(Cp^*Re)_2Co_2(CO)_5B_4H_4$ (**5**). These reaction outcomes are compared and contrasted with those previously observed for 5-sep $(Cp^*Cr_2)_2B_4H_8$.

Introduction

Metallaborane chemistry,[1−3] a part of inorganometallic chemistry,[4] is concerned with compounds containing direct M−B bonding. There are now a large number of metallaboranes known,[5−7] and the electron-counting rules plus the isolobal principle provide a solid foundation for understanding the interrelationships between structure and composition.[8,9] We have synthesized a set of four compounds with the molecular formula $(Cp^*M)_2B_4H_8$ (M = Cr,[10] Re,[11] Ru,[12] Ir;[13] $Cp^* = \eta^5$-C_5Me_5), shown in Chart 1. These compounds both verify the cluster electron-counting ideas and illustrate how the incorporation of an earlier transition metal can lead to electronic unsaturation.[14]

However, even though most of the known metallaboranes are structurally understood, their chemical reactivities remain largely unknown simply because most are isolated from complex systems in low yield. In particular, there is little understanding of how a transition metal can be used to vary the chemistry of a metallaborane. The set of metallaboranes shown in Chart 1 can be prepared conveniently from the reaction of the appropriate Cp^*MCl_n complex with the appropriate monoborane;[15] hence, we have begun to develop a systematic reaction chemistry. The chromium and rhenium compounds have qualitatively similar geometric structures but different electron counts, and the focus of this work is a comparison of their reaction chemistries.

Selected reactions of $(Cp^*Cr)_2B_4H_8$ have been reported earlier, and those pertinent to this work are shown in Scheme 1. Reaction with a source of borane fragments leads to electronically saturated $(Cp^*Cr)_2B_5H_9$.[16] On the other hand, reaction with CO results in the net addition of two CO ligands bound to the Cr centers with the loss of two BHCr bridging hydrogen atoms.[10] The result is a 6-skeletal-electron-pair (6-sep) saturated cluster. Reaction with $Co_2(CO)_8$ leads to the addition of a $Co(CO)_3$ fragment to the hydrogen-bridged face of $(Cp^*Cr)_2B_4H_8$ with loss of one BHCr hydrogen atom.[17] The product, $(Cp^*Cr_2B_4H_7Co(CO)_3$, is viewed as a complex in which the $(Cp^*Cr)_2B_4H_7$ "ligand" supplies 3 electrons to the 15-electron $Co(CO)_3$ fragment and the metal fragment supplies 3 electrons to the $4^1/_2$-sep $(Cp^*Cr)_2B_4H_7$ fragment. In all these

(1) Greenwood, N. N.; Ward, I. M. *Chem. Soc. Rev.* **1974**, *3*, 231.
(2) Housecroft, C. E.; Fehlner, T. P. *Adv. Organomet. Chem.* **1982**, *21*, 57.
(3) Barton, L.; Srivastava, D. K. In *Comprehensive Organometallic Chemistry II*; Abel, E., Stone, F. G. A., Wilkinson, G., Eds.; Pergamon: New York, 1995; Vol. 1.
(4) *Inorganometallic Chemistry*; Fehlner, T. P., Ed.; Plenum: New York, 1992.
(5) Kennedy, J. D. *Prog. Inorg. Chem.* **1984**, *32*, 519.
(6) Kennedy, J. D. *Prog. Inorg. Chem.* **1986**, *34*, 211.
(7) Grimes, R. N. In *Metal Interactions with Boron Clusters*; Grimes, R. N., Ed.; Plenum: New York, 1982; p 269.
(8) Wade, K. *Adv. Inorg. Chem. Radiochem.* **1976**, *18*, 1.
(9) Mingos, D. M. P.; Wales, D. J. *Introduction to Cluster Chemistry*; Prentice Hall: New York, 1990.
(10) Ho, J.; Deck, K. J.; Nishihara, Y.; Shang, M.; Fehlner, T. P. *J. Am. Chem. Soc.* **1995**, *117*, 10292.
(11) Ghosh, S.; Shang, M.; Fehlner, T. P. *J. Organomet. Chem.*, in press.
(12) Lei, X.; Shang, M.; Fehlner, T. P. *J. Am. Chem. Soc.* **1999**, *121*, 1275.
(13) Lei, X.; Shang, M.; Fehlner, T. P. *Organometallics* **2000**, *19*, 118.
(14) Fehlner, T. P. *J. Chem. Soc., Dalton Trans.* **1998**, 1525.
(15) Fehlner, T. P. *Struct. Bonding* **1997**, *87*, 112.
(16) Aldridge, S.; Fehlner, T. P.; Shang, M. *J. Am. Chem. Soc.* **1997**, *119*, 2339.
(17) Aldridge, S.; Hashimoto, H.; Kawamura, K.; Shang, M.; Fehlner, T. P. *Inorg. Chem.* **1998**, *37*, 928.

10.1021/ic0006091 CCC: $19.00
Published on Web 10/21/2000

Chart 1

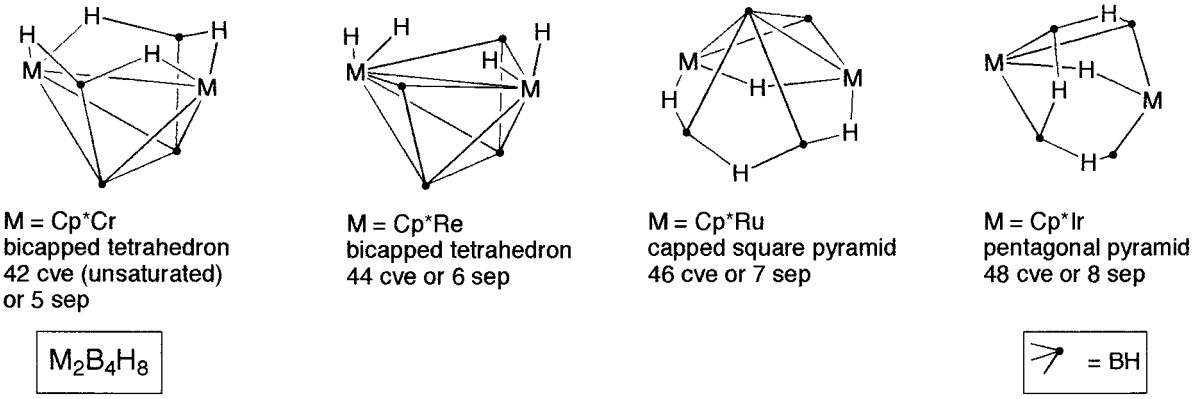

Scheme 1

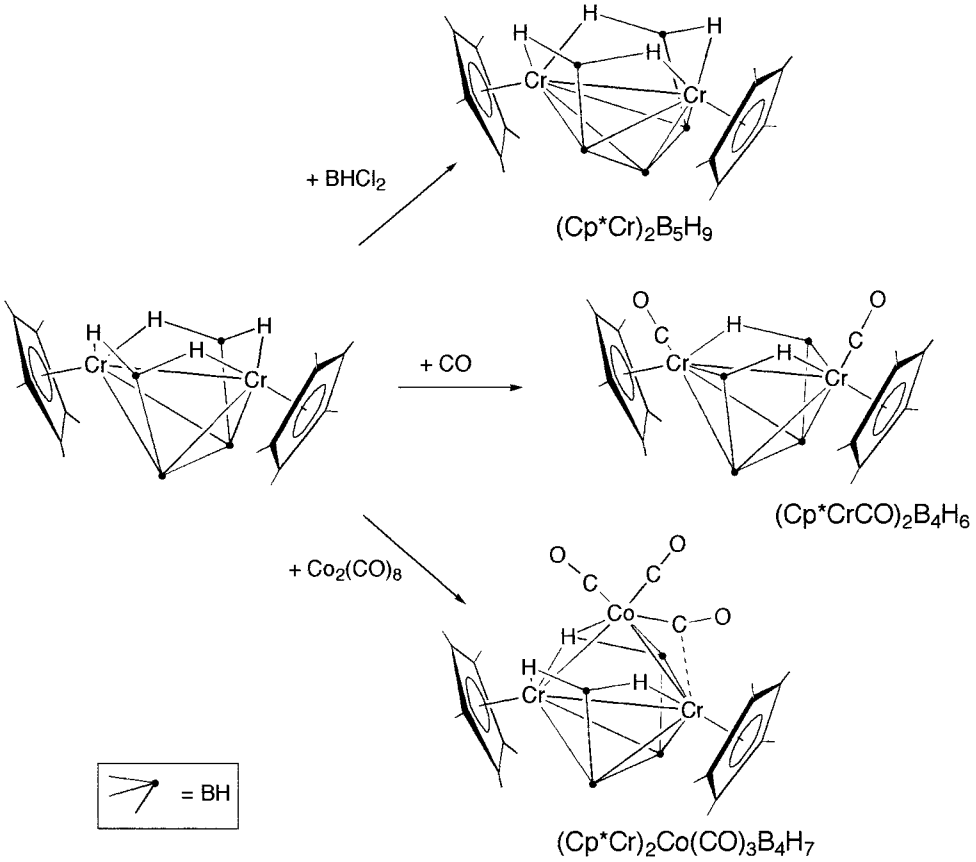

reactions, the driving force appears to be the production of a saturated cluster; however, the reaction rates are disconcertingly slow. Further, the earlier discussion of this chemistry suffered from a lack of any chemistry with which it could be compared.[18] Although it contains a third-row metal, $(Cp^*ReH_2)_2B_4H_4$ (**2**) provides a good comparison, as it has the same geometric structure but a different electron count. Such a comparison should reveal the importance of the transition metal.

The preparation and structure of $(Cp^*ReH_2)_2B_4H_4$ have been described earlier.[11] Although the chromium and rhenium compounds have the same qualitative core geometries, the quantitative differences in geometry correlate well with the frontier orbital energies and characteristics.[11] A key difference involves the four hydrogen atoms associated with the metal centers. The ^{1}H NMR spectra show that, in the chromium compound, these hydrogens are very much borohydride-like (strong coupling to boron, chemical shift in the BHB region) whereas, in the rhenium compound, they are very much metal hydride like (very weak boron coupling, high-field chemical shift). To emphasize this difference, we write $(Cp^*Cr)_2B_4H_8$ vs $(Cp^*ReH_2)_2B_4H_4$.

The reactions of $(Cp^*ReH_2)_2B_4H_4$ (**2**) with BH_3·thf, CO, and $Co_2(CO)_8$ are presented below and compared with those of $(Cp^*Cr)_2B_4H_8$. Some of the results have already been communicated.[19,20] Finally, in conjunction with the CO reaction, we had occasion to revisit the preparative route to **2** and have isolated a hydrogen-rich intermediate. Its presence in the reaction pathway is consistent both with our overall understanding of

(18) Fehlner, T. P. *J. Organomet. Chem.* **1998**, *550*, 21.

(19) Ghosh, S.; Shang, M.; Fehlner, T. P. *J. Am. Chem. Soc.* **1999**, *121*, 7451.

(20) Ghosh, S.; Lei, X.; Cahill, C. L.; Fehlner, T. P. *Angew. Chem., Int. Ed.* **2000**, *39*, 2900.

the reaction of mono(cyclopentadienyl)metal chlorides with monoboranes and with the reaction of **2** with CO.

Experimental Section

General Methods. All the operations were conducted under an Ar atmosphere using standard Schlenk techniques.[21] Solvents were distilled prior to use under N_2. BH_3·thf (1.0 M in THF), $LiBH_4$ (2.0 M in THF), PPh_3, $Fe_2(CO)_9$, $Co_2(CO)_8$, $SiMe_3Cl$ (Aldrich), and $Cp^*Re(CO)_3$ (Strem) were used without further purification. $[Cp^*ReCl_3]_2$ and $[Cp^*ReCl_2]_2$ were prepared according to published procedures,[22] and Cp^*ReCl_4 was prepared by the treatment of Cp^*ReO_3[23] with chlorotrimethylsilane in the presence of triphenylphosphine.[24]

NMR spectra were recorded on 300 and 500 MHz Varian FT-NMR spectrometers. Residual protons of the solvent were used as the reference (benzene δ 7.15), while $[Me_4N(B_3H_8)]$ in acetone-d_6 (δ_B −29.7) contained in a sealed tube was used as the external reference for ^{11}B NMR spectroscopy. Infrared spectra were recorded on a Nicolet 205 FT-IR spectrometer. Mass spectra were obtained on a JEOL JMS-AX505HA mass spectrometer using the EI ionization mode or the FAB mode in a 3-nitrobenzyl alcohol matrix. Perfluorokerosene was used as the standard for the high-resolution EI mass spectra. O_3 gas was generated from an ozone generator (OSMONICS OREC ozone generator, V series), operating at 0.9 A. Elemental analyses were performed by M-H-W Laboratories, Phoenix, AZ.

Synthesis of $(Cp^*ReH_2)_2(B_2H_3)_2$ (1). In a typical reaction, Cp^*ReCl_4 (0.2 g, 0.43 mmol) was loaded into a 100 mL flame-dried Schlenk flask with 15 mL of freshly distilled toluene to generate a purple solution, and the mixture was chilled to −40 °C. $LiBH_4$ (1 mL, 2 mmol) was added very slowly by syringe, and the reaction mixture was allowed to warm to room temperature with stirring. At ∼0 °C, the purple suspension became a greenish-yellow solution accompanied by the evolution of gases. The reaction mixture was then stirred at room temperature for 1 h. Removal of volatiles in vacuo, extraction of the pale yellow residue into hexanes, and filtration afforded a light yellow solution, which on concentration and cooling to −40 °C deposited most of the light-yellow Cp^*ReH_6. Concentration and cooling of the resulting supernatant solution afforded orange-yellow solid **1** (35% based on rhenium).

Spectroscopic Data for 1. Mass (*m*/*z*): MS (EI) P^+(max) 692 (isotopic pattern for 2 Re and 4 B atoms); mass calcd for $^{12}C_{20}{}^1H_{38}{}^{11}B_4{}^{187}Re_2$ 696.2461, obsd 696.2427 (exact mass calculated for M − 2H). ^{11}B NMR (C_6D_6, 22 °C): δ 1.3 (d, J_{B-H} = 166 Hz, 2 B), δ −21.7 (d, J_{B-H} = 151 Hz, 2 B). ^1H NMR (C_6D_6, 22 °C): δ 2.79 (partially collapsed quartet (pcq), 2 BH_t), δ 0.51 (pcq, 2 BH_t), δ 1.95 (s, 30 H, 2 Cp*), δ −2.42 (s, 2 B−H−B), δ −14.58 (s, 4 Re−H- - -B). IR (KBr; cm^{-1}): 2510 w, 2472 w (B−H).

Synthesis of $(Cp^*ReCO)(Cp^*ReH_2)B_4H_4$ (3). Benzene (10 mL) containing 0.05 g (0.07 mmol) of **4** was heated for 5 h at 75 °C, converting the light yellow solution of **4** into a red solution. The reaction mixture was allowed to come to room temperature, solvent was evaporated, and the residue was extracted into hexane. Concentration and cooling of the red extract to −40 °C afforded red **3** (78% yield by NMR). Anal. Calcd for $C_{21}H_{36}Re_2B_4O$: C, 34.26; H, 4.92. Found: C, 34.49; H, 5.01. X-ray-quality crystals were obtained by placing an open 5 mm NMR tube containing a hexane solution of **3** into a Schlenk tube containing a small amount of toluene and maintaining the system at 7 °C.

Spectroscopic Data for 3. Mass (*m*/*z*): MS (EI) P^+(max) 720 (isotopic pattern for 2 Re and 4 B atoms); mass calcd for $^{12}C_{21}{}^1H_{36}{}^{11}B_4{}^{187}Re_2{}^{16}O$ 722.2254, obsd 722.2239. ^{11}B NMR (C_6D_6, 22 °C): δ 87.2 (d, J_{B-H} = 147 Hz, 2 B), δ −11.7 (d, J_{B-H} = 121 Hz, 2 B). ^1H NMR (C_6D_6, 22 °C): δ 9.96 (pcq, 2 BH_t), δ −0.43 (pcq, 2 BH_t), δ 1.92 (s, 15 H, Cp*), δ 1.77 (s, 15 H, Cp*), δ −13.12 (s, 2 Re−H). ^{13}C NMR (C_6D_6, 22 °C): δ 217.6 (Re−CO), δ 97.9, 95.6 (2 Cp* ring), δ 13.1, 10.6 (2 Cp* methyl). IR (KBr; cm^{-1}): 2504 w (B−H), 1926 s (Re−CO).

Synthesis of $(Cp^*ReCO)(Cp^*ReH_2)(B_2H_3)_2$ (4-*cis* and 4-*trans*). CO gas was bubbled through 10 mL of hexane containing 0.12 g (0.17 mmol) of $(Cp^*ReH_2)_2B_4H_4$ for 10 min at room temperature. The reaction flask was closed off, and the contents were stirred for another 5 min. Volatiles were removed in vacuo, the residue was extracted into hexane, and the extract was filtered through Celite. The filtrate was concentrated and stored at −40 °C, whereupon air-sensitive, needle-shaped light yellow crystals of **4** precipitated along with a little Cp^*ReH_6 (total yield 0.09 g, ∼75%). X-ray-quality crystals were obtained by placing an open 5 mm NMR tube containing a hexane solution of **3** into a Schlenk tube containing a small amount of toluene and maintaining the system at 7 °C.

Spectroscopic Data for 4-*cis* and 4-*trans*. Mass (*m*/*z*): MS (EI) P^+(max) 722 (isotopic pattern for 2 Re and 4 B atoms); mass calcd for $^{12}C_{21}{}^1H_{38}{}^{11}B_4{}^{187}Re_2{}^{16}O$ 724.2410, obsd 724.2398. ^{11}B NMR (C_6D_6, 22 °C): δ 13.6 (d, J_{B-H} = 163 Hz, 1 B), δ −1.9 (d, J_{B-H} = 151 Hz, 1 B), δ −7.7 (d, J_{B-H} = 153 Hz, 1 B), δ −20.1 (d, J_{B-H} = 161 Hz, 1 B). ^1H NMR (C_6D_6, 22 °C): δ 2.83 (pcq, 2 BH_t), δ 2.55 (pcq, 2 BH_t), δ −0.15 (pcq, 2 BH_t), δ −0.18 (pcq, 2 BH_t), δ 1.88 (s, 15 H, Cp*), δ 1.85 (s, 15 H, Cp*), δ 1.84 (s, 15 H, Cp*), δ 1.82 (s, 15 H, Cp*), δ −2.01 (br s, 4 B−H−B), δ −12.55 (br s, 2 B−H−Re), δ −14.42 (s, 2 Re−H). ^{13}C NMR (C_6D_6, 22 °C): δ 206.7, 204.1 (Re−CO, cis and trans isomers); δ 95.9, 94.5, 92.4, 89.2 (4 Cp* rings); δ 13.1, 13.04, 12.3, 11.7 (4 Cp* methyl). IR (KBr; cm^{-1}): 2510 w, 2472 w (B−H), 1923 s (trans Re−CO), 1889 s (cis Re−CO).

Synthesis of $(Cp^*Re)_2Co_2(CO)_5B_4H_4$ (5). To a 100 mL Schlenk tube containing 0.07 g (0.1 mmol) of $(Cp^*ReH_2)_2B_4H_4$ in 10 mL of hexane was added 0.06 g (0.2 mmol) of solid $Co_2(CO)_8$. Immediately after the addition of $Co_2(CO)_8$, the color changed from yellow to deep brown with the evolution of gases. After 15 min, solvent was evaporated and the solid was extracted into hexane. The extract was concentrated, and brown $Co_4(CO)_{12}$ was removed by fractional crystallization at −40 °C. The mother liquor was concentrated and quickly passed through a small silica gel column to yield a yellowish brown solution. This solution was concentrated and stored at −40 °C overnight, whereupon two types of crystals formed. The brown $(Cp^*Re)_2Co_2(CO)_5B_4H_4$ crystals were manually separated from the $Cp^*Re(CO)_3$ crystals (presumably resulting from the impurity of Cp^*ReH_6 in $(Cp^*ReH_2)_2B_4H_4$) and recrystallized at −4 °C. The total yield (NMR) of $(Cp^*Re)_2Co_2(CO)_5B_4H_4$ was ∼75%; however, the compound was not analytically pure.

Spectroscopic Data for 5. Mass (*m*/*z*): MS (EI) P^+(max) 949 (isotopic pattern for 2 Re and 4 B atoms); mass calcd for $^{12}C_{25}{}^1H_{34}{}^{11}B_4{}^{187}Re_2{}^{59}Co_2{}^{16}O_5$ 950.0558, obsd 950.0586. ^{11}B NMR (C_6D_6, 22 °C): δ 87.8 (d, J_{B-H} = 172 Hz, 2 B), δ 86.7 (d, J_{B-H} = 162 Hz, 2 B). ^1H NMR (C_6D_6, 22 °C): δ 9.31 (pcq, 2 BH_t), δ 4.38 (pcq, 2 BH_t), δ 1.67 (s, 30 H, 2 Cp*). IR (KBr; cm^{-1}): 2536 w, 2453 w (B−H_t), 2022 s (Co−CO), 1997 vs (Co−CO), 1972 s (Co−CO), 1820 w (Co−(μ-CO)).

Relaxation Measurements. The longitudinal relaxation times were measured for Re−H hydrogens in a mixture of **1**, **2**, and Cp^*ReH_6 over the temperature range +22 to −80 °C in toluene-d_8 using standard methods. At −80 °C, 415 ms (eq) and 221 ms (ax) were observed for Cp^*ReH_6, vs 618 and 290 ms reported previously at 30 °C in the same solvent.[25] The values 120 and 109 ms were observed for **1** and **2**, respectively, at the same temperature.

X-ray Structure Determinations. Details of the data collection and structure refinement procedures for compounds **3**−**5** are summarized in Table 1. Data collections for compounds **3** and **4** were carried out on a Bruker SMART CCD diffractometer, and that for **5** was carried out on an Enraf-Nonius CAD 4 diffractometer.

(a) $(Cp^*ReCO)(Cp^*ReH_2)B_4H_4$ (3). A dark red crystal of **3** was grown by slow evaporation of a hexane solution over a period of 10 days. This crystal, a hexagonal plate, 0.21 × 0.21 × 0.04 mm^3, was attached to a glass fiber and mounted on a Bruker SMART CCD diffractometer for data collection at 294 K. A hemisphere of intensity data were collected using Mo Kα X-rays, a crystal-to-detector distance

(21) Shriver, D. F.; Drezdzon, M. A. *The Manipulation of Air-Sensitive Compounds*, 2nd ed.; Wiley-Interscience: New York, 1986.
(22) Herrmann, W. A.; Fischer, R. A.; Herdtweck, E. *J. Organomet. Chem.* **1987**, *329*, C1.
(23) Gable, K. P.; Phan, T. N. *J. Organomet. Chem.* **1994**, *466*, C5.
(24) Herrmann, W. A.; Herdtweck, E.; Floel, M.; Kulpe, J.; Kusthardt, U.; Okuda, J. *Polyhedron* **1987**, *6*, 1165.
(25) Hamilton, D. G.; Crabtree, R. H. *J. Am. Chem. Soc.* **1988**, *110*, 4126.

Table 1. Crystal Data and Structure Refinement Details for Compounds **3**−**5**

	4	**3**	**5**
empirical formula	$C_{21}H_{38}B_4ORe_2$	$C_{21}H_{36}B_4ORe_2$	$C_{25}H_{34}B_4Co_2O_5Re_2$
crystal system	monoclinic	monoclinic	orthorhombic
space group	$P2_1/c$	$P2_1/c$	$Pbca$
temp (K)	293(2)	293(2)	293(2)
wavelength (Å)	0.710 73	0.710 73	0.710 73
fw	722.15	720.14	948.02
a (Å)	16.1604(10)	8.1687(9)	23.282(2)
b (Å)	14.9037(10)	14.575(2)	16.787(2)
c (Å)	20.2280(13)	20.674(2)	15.0481(14)
α (deg)	90	90	
β (deg)	98.1780(10)	100.770(2)	
γ (deg)	90	90	
V (Å^3)	4822.4(5)	2418.1(5)	5881.3(10)
Z	8	4	8
ρ(calcd) (Mg/m^3)	1.989	1.978	2.141
abs coeff (mm^{-1})	10.041	10.012	9.347
F(000)	2616	1360	3584
crystal size (mm^3)	0.48 × 0.10 × 0.07	0.21 × 0.21 × 0.04	0.55 × 0.07 × 0.06
θ range (deg)	1.70−28.30	1.70−28.30	2.02−24.99
index ranges	$-18 \le h \le 19$	$-10 \le h \le 5$	$-27 \le h \le 0$
	$-17 \le k \le 14$	$-17 \le k \le 18$	$0 \le k \le 19$
	$-24 \le l \le 23$	$-26 \le l \le 27$	$0 \le l \le 17$
no. of reflns collected	26 101	12 522	5168
no. of independent reflns [R(int)]	8398 [0.1174]	4240 [0.1051]	
abs cor	semiempirical	analytical	ψ scan
max and min transm	0.7945 and 0.3546	0.696 08 and 0.170 46	0.7710 and 0.7104
refinement method	full-matrix least-squares on F^2	full-matrix least-squares on F^2	full-matrix least-squares on F^2
no. of data/restraints/parameters	8398/0/505	4186/0/253	5168/0/344
goodness-of-fit on F^2	0.893	0.918	1.000
final R indices [$I > 2\sigma(I)$]: R1, wR2	0.0470, 0.0985	0.0500, 0.1042	0.0368, 0.0757
largest diff peak and hole (e Å^{-3})	3.829 and −1.776	2.976 and −2.479	0.992 and −0.977

of 5.0 cm, and 0.3° steps in ω. The unit cell was refined from 2840 strong reflections using least-squares techniques. The data were reduced and corrected for Lorentz, polarization, and background effects via the Bruker program SAINT.[26] An analytical absorption correction was performed with XPREP[27] using six indexed faces. A total of 12 522 reflections were collected, of which 4240 were unique [R(int) = 0.1051]. Structure solution proceeded by direct methods,[28] and subsequent refinements were carried out using SHELXTL-98.[29] The hydrogen atoms of the Cp* group were refined isotropically with an idealized riding model, while the B−H and Re−H hydrogen atoms were not found and thus were not included in the final refinement. Graphics and tables were produced using the WINGX[30] suite of programs. Selected bond distances and bond angles for the compound are listed in Table 2; other crystallographic data have been deposited as Supporting Information in conjunction with the original communication.[20]

(b) (Cp*ReCO)(Cp*ReH$_2$)(B$_2$H$_3$)$_2$ (4-*cis* and 4-*trans*). A light yellow, thin, needlelike crystal of **4** was grown by slow evaporation of a hexane solution over a period of 6 days. This crystal, 0.48 × 0.10 × 0.07 mm^3, was attached to a glass fiber and mounted on a Bruker SMART CCD diffractometer for data collection at 294 K. A hemisphere of intensity data were collected using Mo Kα X-rays, a crystal-to-detector distance of 5.0 cm, and 0.3° steps in ω. The unit cell was refined from 6086 strong reflections using least-squares techniques. The data were reduced and corrected for Lorentz, polarization, and background effects via the Bruker program SAINT.[26] An empirical absorption correction was performed by modeling the crystal as a (010) plate and discarding reflections with plate-glancing angles of less than 3.0°. This reduced the R(int) of 3751 reflections with $I > 15\sigma$ from 0.12 to 0.092. A total of 26 101 reflections were collected, of which 8398 were unique [R(int) = 0.1174]. Structure solution proceeded by direct methods,[2] and subsequent refinements were carried out using SHELXTL-98.[29] The hydrogen atoms of the Cp* group were refined isotropically with an idealized riding model, while the B−H and Re−H hydrogen atoms were not found and thus were not included in the final refinement. Graphics and tables were produced using the WINGX[30] suite of programs. Selected bond distances and bond angles are listed in Table 3; other crystallographic data have been deposited as Supporting Information in conjunction with the original communication.[20]

Table 2. Selected Bond Distances (Å) and Bond Angles (deg) for (Cp*ReH$_2$)(Cp*ReCO)B$_4$H$_4$ (**3**)

Re(1)−B(1)	2.11(2)	Re(2)−B(2)	2.29(2)
Re(1)−B(2)	2.17(2)	Re(2)−C(13)	2.300(14)
Re(1)−C(1)	2.22(2)	Re(2)−B(3)	2.39(2)
Re(1)−B(4)	2.26(2)	B(1)−B(2)	1.85(3)
Re(1)−C(4)	2.28(2)	B(2)−B(3)	1.70(3)
Re(1)−B(3)	2.28(2)	B(3)−B(4)	1.67(3)
Re(1)−Re(2)	2.7819(8)	Re(2)−C(14)	2.326(14)
Re(2)−B(1)	2.12(2)	C(21)−O(21)	1.14(2)
Re(2)−B(4)	2.17(2)	C(1)−C(5)	1.29(3)
Re(2)−C(11)	2.24(2)	C(1)−C(2)	1.46(3)
Re(2)−C(12)	2.26(2)	C(3)−C(4)	1.36(3)

B(1)−Re(1)−B(2)	51.3(8)	B(1)−Re(1)−B(3)	88.1(8)
B(1)−Re(1)−C(1)	142.0(8)	B(2)−Re(1)−C(2)	107.4(10)
B(2)−Re(1)−C(1)	144.3(9)	B(2)−Re(1)−B(3)	44.8(8)
B(1)−Re(1)−B(4)	98.8(6)	B(4)−Re(1)−B(3)	43.1(7)
B(2)−Re(1)−B(4)	80.1(8)	B(1)−Re(2)−B(2)	49.4(8)
B(1)−Re(1)−Re(2)	49.2(4)	B(1)−Re(2)−B(2)	49.4(8)
B(2)−Re(1)−Re(2)	53.4(5)	B(4)−Re(2)−B(2)	79.4(7)
B(4)−Re(1)−Re(2)	49.7(5)	B(4)−Re(2)−C(13)	92.7(7)
B(3)−Re(1)−Re(2)	55.3(5)	B(1)−Re(2)−B(3)	84.9(8)
B(1)−Re(2)−B(4)	101.1(7)	B(4)−Re(2)−B(3)	42.5(7)
B(1)−Re(2)−C(11)	97.0(10)	B(2)−Re(2)−B(3)	42.5(7)
B(1)−Re(2)−Re(1)	48.6(5)	O(21)−C(21)−Re(2)	173.5(16)
B(4)−Re(2)−Re(1)	52.5(5)	Re(1)−B(1)−Re(2)	82.2(7)
B(2)−Re(2)−Re(1)	49.5(4)	B(3)−B(2)−B(1)	108.7(14)
B(3)−Re(2)−Re(1)	51.7(5)	B(3)−B(2)−Re(1)	71.1(10)
B(2)−B(1)−Re(1)	66.1(9)	B(1)−B(2)−Re(1)	62.6(8)
B(2)−B(1)−Re(2)	69.9(9)	B(4)−B(3)−B(2)	115.8(16)

(c) (Cp*Re)$_2$B$_4$H$_4$Co$_2$(CO)$_5$ (5). A needlelike dark brown crystal of **5** was grown by the slow evaporation of a hexane solution at 4 °C

(26) Bruker, A. *SAINT*; Bruker: Madison, WI, 1998.
(27) Bruker, A. *XPREP*; Bruker: Madison, WI, 1998.
(28) Sheldrick, G. M. *Acta Crystallogr* **1990**, *A46*, 467.
(29) Bruker, A. *SHELXTL-98*; Bruker: Madison, WI, 1998.
(30) Farrugia, L. J. *WINGX*; University of Glasgow: Glasgow, U.K., 1998.

Table 3. Selected Bond Distances (Å) and Bond Angles (deg) for $(Cp^*ReH_2)(Cp^*ReCO)B_4H_6$ (**4**)

Re(1)−B(4)	2.205(16)	Re(2)−B(2)	2.355(16)
Re(1)−B(3)	2.178(15)	B(1)−B(2)	1.72(3)
Re(1)−B(2)	2.213(17)	B(3)−B(4)	1.63(2)
Re(1)−C(4)	2.271(11)	C(1)−C(2)	1.422(18)
Re(1)−C(5)	2.269(11)	Re(3)−B(5)	2.158(14)
Re(1)−C(3)	2.271(13)	Re(1)−B(4)	2.205(16)
Re(1)−C(1)	2.293(13)	Re(3)−B(8)	2.125(18)
Re(1)−B(1)	2.376(19)	Re(3)−C(22)	2.266(13)
Re(1)−Re(2)	2.7730(7)	Re(3)−B(6)	2.417(15)
Re(2)−B(1)	2.235(15)	Re(3)−B(7)	2.336(18)
Re(2)−B(4)	2.194(15)	Re(3)−Re(4)	2.8274(7)
Re(2)−B(3)	2.264(17)	Re(4)−B(8)	2.298(16)
Re(4)−B(5)	2.219(16)	Re(4)−B(6)	2.29(2)
Re(4)−B(7)	2.314(14)	B(5)−B(6)	1.72(3)
B(7)−B(8)	1.70(3)	C(42)−O(42)	1.200(14)

B(3)−Re(1)−B(4)	43.7(7)	B(4)−Re(1)−B(2)	96.1(6)
B(3)−Re(1)−B(2)	63.4(7)	B(2)−Re(1)−B(1)	43.8(7)
B(4)−Re(1)−C(4)	142.0(5)	B(1)−Re(2)−Re(1)	55.4(5)
B(3)−Re(1)−C(4)	145.4(6)	B(4)−Re(1)−Re(2)	50.8(4)
B(2)−Re(1)−C(5)	151.0(5)	B(3)−Re(1)−Re(2)	52.8(4)
C(4)−Re(1)−C(2)	59.0(5)	B(2)−Re(1)−Re(2)	55.0(4)
B(4)−Re(1)−B(1)	100.6(5)	B(1)−Re(1)−Re(2)	50.7(3)
B(3)−Re(1)−B(1)	93.8(6)	B(1)−Re(2)−B(4)	105.5(6)
Re(1)−B(3)−Re(2)	77.2(5)	B(4)−Re(2)−Re(1)	51.1(4)
B(1)−Re(2)−B(3)	95.4(7)	B(3)−Re(2)−Re(1)	50.0(4)
B(4)−Re(2)−B(3)	42.9(6)	B(2)−B(1)−Re(2)	71.8(8)
B(3)−Re(2)−B(2)	59.9(7)	B(2)−B(1)−Re(1)	63.1(9)
B(1)−Re(2)−B(2)	43.9(8)	Re(2)−B(1)−Re(1)	73.9(5)
B(4)−Re(2)−B(2)	92.4(6)	Re(1)−B(2)−Re(2)	74.7(5)
B(5)−Re(4)−B(7)	101.7(6)	B(8)−Re(4)−Re(3)	47.6(4)
B(5)−Re(3)−B(6)	43.7(6)	B(5)−Re(4)−Re(3)	48.8(4)
B(8)−Re(3)−B(6)	104.1(6)	B(6)−B(5)−Re(3)	76.1(7)
B(5)−Re(3)−B(8)	86.1(7)	B(6)−B(5)−Re(4)	69.9(8)
B(5)−Re(3)−B(7)	102.9(6)	Re(3)−B(8)−Re(4)	79.4(6)
B(8)−Re(3)−B(7)	44.4(7)	B(8)−B(7)−Re(3)	61.2(8)
B(8)−Re(4)−B(5)	80.5(5)	O(42)−C(42)−Re(4)	172.5(11)

in a small Schlenk tube. This crystal, having approximate dimensions of 0.45 × 0.07 × 0.06 mm,[3] was mounted on a glass fiber in a random orientation. The compound was found to crystallize in the orthorhombic space group *Pbca*, with the cell parameters $a = 23.282(2)$ Å, $b = 16.787(2)$ Å, $c = 15.0481(14)$ Å, and $V = 5881.3(10)$ Å^3. Preliminary examination and data collection were performed with Mo Kα radiation ($\lambda = 0.710\,73$ Å) on an Enraf-Nonius CAD4 computer-controlled κ axis diffractometer equipped with a graphite-crystal, incident-beam monochromator. Structure solution and refinement were performed on a PC by using the SHELXTL-94 package.[31] Most of the non-hydrogen atoms were located by direct methods; the remaining non-hydrogen atoms were found in succeeding difference Fourier syntheses. Least-squares refinement was carried out on F^2 for all reflections. After all non-hydrogen atoms were refined anisotropically, difference Fourier syntheses located all hydrogen atoms. However, in the final refinement, pentamethylcyclopentadienyl hydrogen atoms were refined with an idealized riding model that restrained the C−H distance to 0.96 Å and the isotropic thermal parameter of a hydrogen atom to 1.5 times of the equivalent isotropic thermal parameter of its bonded carbon atom, while the respective parameters for restraining borane hydrogen atoms were 1.10 Å and 1.2. Selected bond distances and bond angles are listed in Table 4; other crystallographic data have been deposited as Supporting Information in conjunction with the original communication.[19]

Results and Discussion

A summary of the reactions of Cp^*ReCl_n, $n = 2-4$, with $LiBH_4$ is given in Scheme 2, and the reactions of $(Cp^*ReH_2)_2B_4H_4$ (**2**) with BH_3·thf, CO, and $Co_2(CO)_8$ are summarized in Schemes 3−5. The latter may be compared with similar reactions for $(Cp^*Cr)_2B_4H_8$ in Scheme 1. Each reaction type is treated separately in the following.

(31) Sheldrick, G. M. *SHELXTL-94*; Siemens: Madison, WI, 1994.

Table 4. Selected Bond Distances (Å) and Bond Angles (deg) for *closo*-$(Cp^*Re)_2\{\mu\text{-}\eta^6\text{:}\eta^6\text{-}B_4H_4Co_2(CO)_5\}$ (**5**)

Re(1)−B(3)	2.130(10)	Re(2)−B(1)	2.237(10)
Re(1)−B(2)	2.150(11)	Re(2)−B(4)	2.255(11)
Re(1)−B(1)	2.189(10)	Re(2)−Co(2)	2.6157(12)
Re(1)−B(4)	2.194(11)	Re(2)−Co(1)	2.6460(12)
Re(1)−Re(2)	2.6393(5)	Co(1)−B(1)	2.010(11)
Re(1)−Co(1)	2.6478(12)	Co(1)−Co(2)	2.4192(17)
Re(1)−Co(2)	2.6854(13)	Co(2)−B(4)	2.036(11)
Re(2)−B(3)	2.142(10)	B(1)−B(2)	1.712(15)
Re(2)−B(2)	2.161(10)	B(2)−B(3)	1.770(15)
B(3)−H(3)	1.1000	B(3)−B(4)	1.712(15)

B(3)−Re(1)−B(2)	48.8(4)	B(2)−Re(2)−B(4)	87.6(4)
B(2)−Re(1)−B(1)	46.4(4)	B(3)−Re(2)−Co(2)	91.0(3)
B(3)−Re(1)−B(4)	46.6(4)	B(2)−Re(2)−Co(2)	113.5(3)
B(2)−Re(1)−B(4)	89.5(4)	B(1)−Re(2)−Co(2)	94.0(3)
B(3)−Re(1)−Re(2)	52.0(3)	B(3)−Re(2)−Re(1)	51.6(3)
B(2)−Re(1)−Re(2)	52.4(3)	B(2)−Re(2)−Re(1)	52.1(3)
B(1)−Re(1)−Re(2)	54.2(3)	B(1)−Re(2)−Re(1)	52.6(3)
B(4)−Re(1)−Re(2)	54.7(3)	B(4)−Re(2)−Re(1)	52.6(3)
B(3)−Re(1)−Co(1)	112.1(3)	Co(2)−Re(2)−Re(1)	61.46(3)
B(2)−Re(1)−Co(1)	90.0(3)	B(3)−Re(2)−Co(1)	111.8(3)
B(1)−Re(1)−Co(1)	47.9(3)	B(2)−Re(2)−Co(1)	89.8(3)
B(4)−Re(1)−Co(1)	94.7(3)	B(4)−Re(2)−Co(1)	93.3(3)
Re(2)−Re(1)−Co(1)	60.06(3)	Co(2)−Re(2)−Co(1)	54.74(4)
B(3)−Re(1)−Co(2)	89.4(3)	Re(1)−Re(2)−Co(1)	60.13(3)
B(2)−Re(1)−Co(2)	111.3(3)	B(1)−Co(1)−Co(2)	106.5(3)
B(3)−Re(2)−B(2)	48.6(4)	B(4)−Co(2)−Co(1)	106.4(3)
B(3)−B(2)−Re(1)	65.0(5)	B(2)−B(1)−Re(2)	64.8(5)
B(1)−B(2)−Re(2)	69.4(5)	Co(1)−B(1)−Re(2)	76.9(3)
Re(1)−B(2)−Re(2)	75.5(3)	Re(1)−B(1)−Re(2)	73.2(3)

Isolation of a Precursor to $(Cp^*ReH_2)_2B_4H_4$ (2). The reaction between Cp^*ReCl_4 and $LiBH_4$ at low temperature yields a mixture of two products. The major product contains no boron and is identified as the known hydride Cp^*ReH_6.[32] The other product isolated is a metallaborane with the composition $(Cp^*Re)_2B_4H_{10}$ (**1**). Thermolysis of **1** cleanly leads to **2**. Attempts to obtain an X-ray-quality crystal of **1** were unsuccessful because the compound cocrystallizes with **2**, which continuously forms from **1** even at room temperature. Compound **1** is also observed in the reaction of Cp^*ReCl_4 with BH_3·thf, albeit in comparatively lower yield.

Despite the lack of a solid-state structure, the spectroscopic data provide considerable information on the cage connectivity. On the basis of ^{11}B NMR spectroscopy, compound **1** possesses two types of BH fragments in a ratio of 1:1. The ^{1}H NMR spectrum shows two types of BH terminal protons in accord with the ^{11}B spectrum, one type of Cp* methyl protons, one type of BHB protons, and one type of ReH protons (small coupling to boron) in the ratio of 1:1:15:1:2. The spectrum is independent of temperature (−80 °C to room temperature). The assignments and coupling patterns have been confirmed by ^{1}H{selective ^{11}B} NMR spectroscopy. On the basis of the NMR data combined with the mass spectrometric information, the compound is formulated as 7-sep $(Cp^*ReH_2)_2(B_4H_6)$. The presence of two hydrogen atoms on each rhenium center led us to investigate the ^{1}H relaxation times as a function of temperature.[33−35] The values for both **1** and **2** are less than half those for Cp^*ReH_6 at the lowest temperature (−80 °C). However, the low values are most likely caused by the small, but real, interaction with the quadrupolar boron nuclei rather than by H−H bonding.

(32) Herrmann, W. A.; Okuda, J. *Angew. Chem., Int. Ed. Engl.* **1986**, *25*, 1092.
(33) Hlatky, G. G.; Crabtree, R. H. *Coord. Chem. Rev.* **1985**, *85*, 1.
(34) Kubas, G. J.; Ryan, R. R.; Swanson, B. I.; Vergamini, P. J.; Wasserman, J. J. *J. Am. Chem. Soc.* **1984**, *106*, 451.
(35) Kubas, G. J.; Ryan, R. R.; Wrobleski, D. A. *J. Am. Chem. Soc.* **1986**, *108*, 1339.

Scheme 2

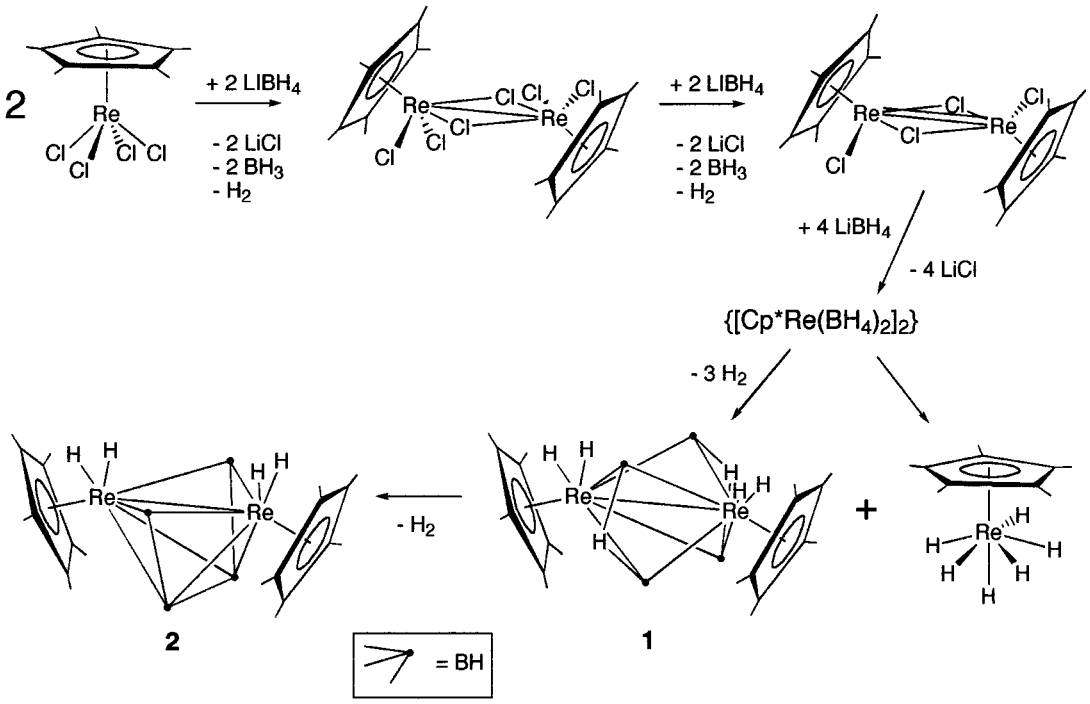

Scheme 3

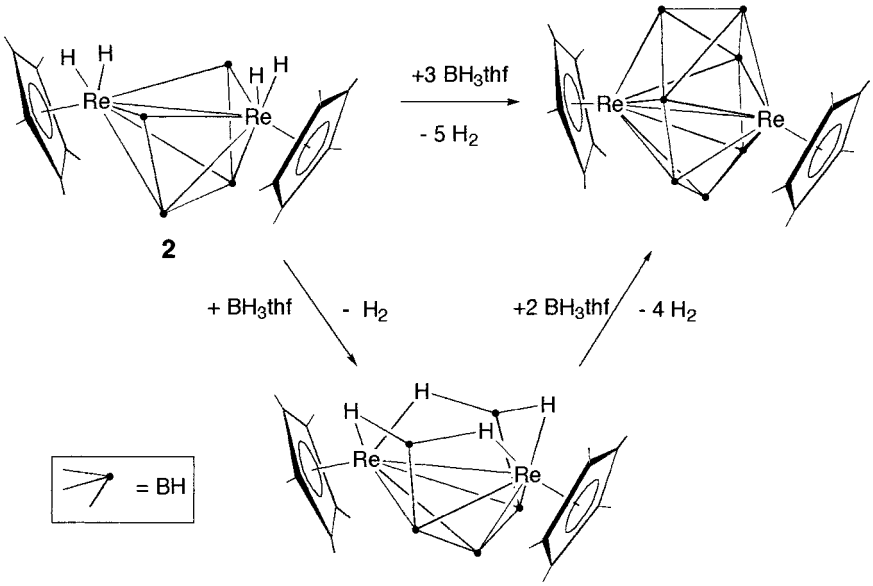

The sep count is consistent with an octahedral, capped square pyramidal, or edge-sharing bitetrahedral cluster structure. From a comparison of the chemical shifts with those of $(Cp^*Ru)_2B_4H_8$, having a known capped square pyramidal structure (Chart 1),[12] this structure is ruled out.[36] An octahedral structure is possible but considered unlikely. Hence, we postulate an M−M edge-sharing bitetrahedral structure for **1** similar to those of 7-sep $(Cp^*Mo)_2(B_2H_6)_2$ and $(Cp^*W)_2(B_2H_6)_2$.[37,38] The analysis of 7-sep $(Cp^*ReCO)(Cp^*ReH_2)(B_2H_3)_2$ (**4**), structurally characterized in the solid state and discussed below, corroborates the structural assignment. Hence, **1** is formulated as $(Cp^*Re_2H_2)_2(B_2H_3)_2$. Hydrogen-rich intermediates along the synthetic pathway have been observed previously in both the tungsten and iridium systems.[38,39]

Formation of 1 from Cp^*ReCl_4. It is our contention that the metal nuclearity of the Cp^*MCl_n complex determines the metal nuclearity of the metallaborane product; e.g., Cp^*WCl_4 yields a mononuclear product whereas $[Cp^*WCl_2]_2$ yields a dinuclear product.[38] However, net reduction of the metal center can be more rapid than metallaborane formation; e.g., both Cp^*MoCl_4 and $[Cp^*MoCl_2]_2$ yield dinuclear products.[37] As both Cp^*ReCl_3 and Cp^*ReCl_2 are dimeric species, we investigated the viability of each as a precursor in the formation of **1** from Cp^*ReCl_4.[22]

(36) Fehlner, T. P. *Collect. Czech. Chem. Commun.* **1999**, *64*, 767.
(37) Aldridge, S.; Shang, M.; Fehlner, T. P. *J. Am. Chem. Soc.* **1998**, *120*, 2586.
(38) Weller, A. S.; Shang, M.; Fehlner, T. P. *Organometallics* **1999**, *18*, 53.
(39) Lei, X.; Shang, M.; Fehlner, T. P. *Chem.—Eur. J.* **2000**, *6*, 2653.

Scheme 4

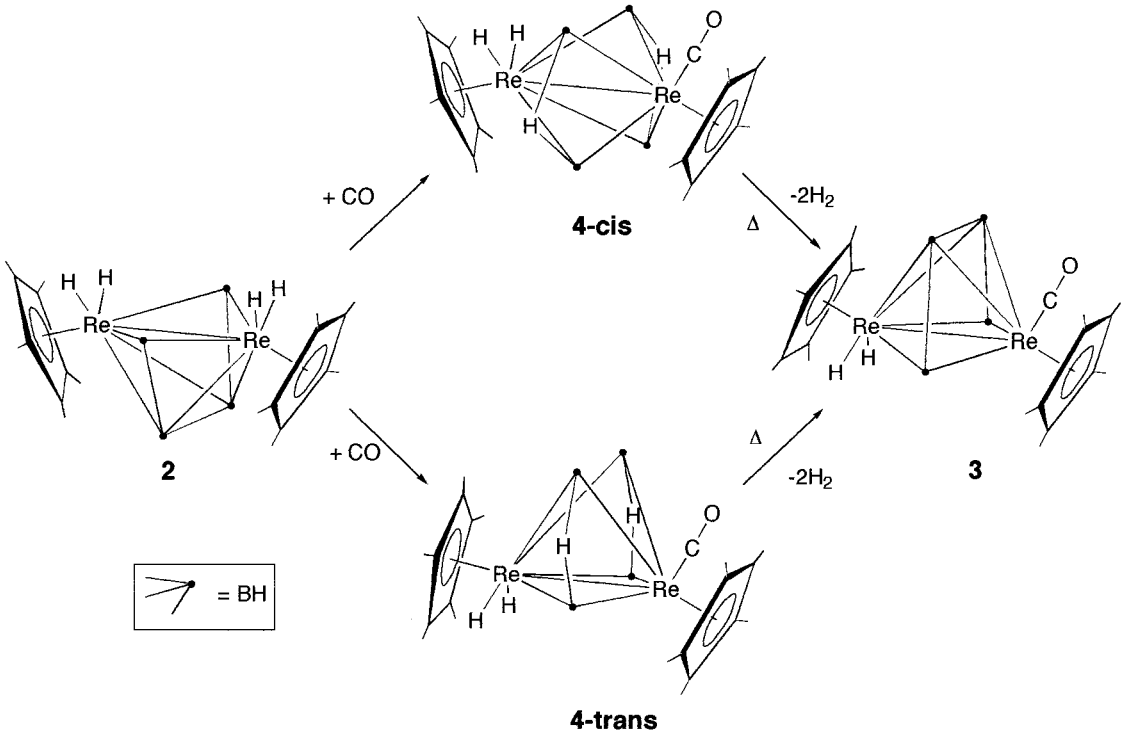

Scheme 5

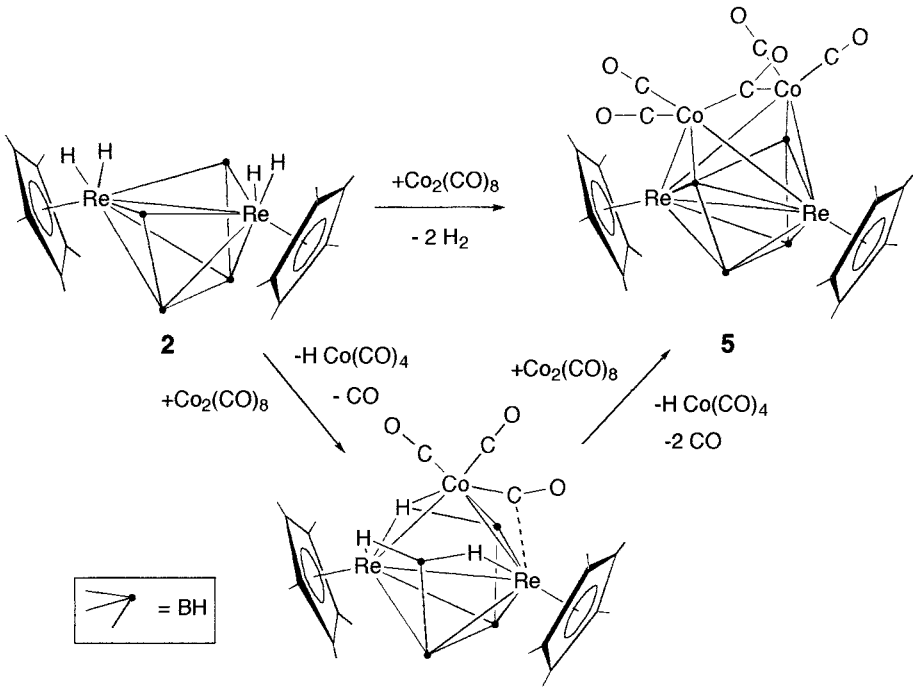

Thus, the reactions of both brown $[Cp^*ReCl_3]_2$ and green $[Cp^*ReCl_2]_2$ with $LiBH_4$ have been studied by ^{11}B NMR. In each case, the formation of **1** is observed. As the reaction of Cp^*ReCl_4 (purple) with $LiBH_4$ proceeds through a greenish yellow stage, reduction to $[Cp^*ReCl_2]_2$ via loss of BH_3 and H_2 from the borohydride is more rapid than H_2 elimination and metallaborane formation. Hence, we suggest that **1** appears to be formed via the putative $[Cp^*Re(BH_4)_2]_2$ intermediate, as shown in Scheme 2. Unfortunately, Cp^*ReH_6 also arises in this step. Thus far, we have been unable to suppress the hydride formation. The hydride may be accompanied by a monorhenium metallaborane; however, we were unable to isolate such a compound although some unidentified signals were observed in the ^{11}B NMR spectrum of the reaction mixture. In support of this supposition, note that the reaction of $[Cp^*IrCl_2]_2$ with $LiBH_4$ yields $Cp^*IrH_2B_3H_7$ and Cp^*IrH_4.[40]

Reaction of $(Cp^*ReH_2)_2B_4H_4$ with BH_3·thf. The reaction between **2** and excess BH_3·thf at 65 °C leads to the clean formation of 7-sep $(Cp^*Re)_2B_7H_7$, a hypoelectronic metallaborane, which was fully described previously (Scheme 3).[41,42] $(Cp^*Re)_2B_7H_7$ was isolated from the reaction between Cp^*ReCl_4

(40) Lei, X.; Bandyopadhyay, A. K.; Shang, M.; Fehlner, T. P. *Organometallics* **1999**, *18*, 2294.
(41) Weller, A. S.; Shang, M.; Fehlner, T. P. *Chem. Commun.* **1998**, 1787.

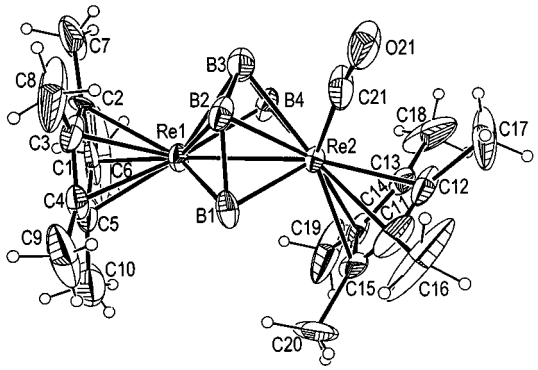

Figure 1. Molecular structure of $(Cp^*ReH_2)(Cp^*ReCO)B_4H_4$ (**3**).

and excess BH_3·thf with heating. The origin of $(Cp^*Re)_2B_7H_7$ in this reaction is now clear. Use of $LiBH_4$ as the monoboron reagent limits the number of boron atoms in the metallaborane product to the number of chlorides in the Cp^*ReCl_x species that is stable with respect to reduction—$[Cp^*ReCl_2]_2$ yields **2** via **1** (Scheme 2). Borane, on the other hand, is thought to generate the same key borohydride, but if borane is present in sufficient excess at the proper temperature, it can add to the first formed metallaborane to increase the size of the borane fragment—$[Cp^*ReCl_2]_2$ yields **2** via **1** and on heating yields $(Cp^*Re)_2B_7H_7$. This is fully consistent with systems we have investigated previously; e.g., the reaction of $[Cp^*MoCl_2]_2$ with $LiBH_4$ yields $(Cp^*Mo)_2(B_2H_6)_2$, but the reaction with BH_3·thf yields $(Cp^*Mo)B_5H_9$.[37]

Compare these observations for **2** with those for the 5-sep $(Cp^*Cr)_2B_4H_8$ metallaborane (Scheme 1). First, reaction with borane ceases after the formation of $(Cp^*Cr)_2B_5H_9$.[17] Second, in contrast to the rhenium system, the reaction is very slow. Reaction with BH_3·thf is incomplete despite extended reaction times (3 weeks), and the more active compound $BHCl_2$ must be used for more efficient addition. Note that the environment of the metal in $(Cp^*Cr)_2B_5H_9$ is very similar to that in $(Cp^*Cr)_2B_4H_8$. Thus, we suggest that $(Cp^*Re)_2B_5H_9$ may be an intermediate in the formation of $(Cp^*Re)_2B_7H_7$ and that it is the difference in the character of the four extra hydrogens that generates the difference in reactivity. All four endo-hydrogens in $(Cp^*ReH_2)_2B_4H_4$ are replaced, but the Cr analogue retains all these hydrogens. The very different environments of these hydrogens as reflected in the NMR chemical shifts are also reflected in the relative reactivities of the two compounds.

Reaction of $(Cp^*ReH_2)_2B_4H_4$ with CO. Mild heating of **2** with 1 atm of CO leads to the formation of the 6-sep metallaborane $(Cp^*ReH_2)(Cp^*ReCO)B_4H_4$ (**3**), in which a net substitution of two rhenium hydrides by CO has taken place (Scheme 4). The spectroscopic data are consistent with this conclusion. In particular, the IR spectrum shows a single terminal CO stretch and the ^1H NMR spectrum shows an ReH resonance corresponding to 2 H. The core structure was confirmed by a solid-state structure determination and is shown in Figure 1; crystal data and geometric parameters are given in Tables 1 and 2. The hydrogen atoms were not located, but their bonding partners are clearly defined by the NMR spectra. The core structure of **3** is almost identical with that of **2**, e.g., Re—Re bond distances of 2.7819(8) Å in **3** and 2.8091(8) Å in **2**.[11] The bicapped tetrahedral geometry is retained; however, there is one difference that becomes important below. Although **2** has a cisoid disposition of the Cp* ligands and, consequently, the rhenium hydrides, **3** has a transoid disposition of the Cp* ligands, thereby placing the CO ligand adjacent to the central B—B bond of the B_4 fragment. Contrast this arrangement with that of $(Cp^*CrCO)_2B_4H_6$ shown in Scheme 1.

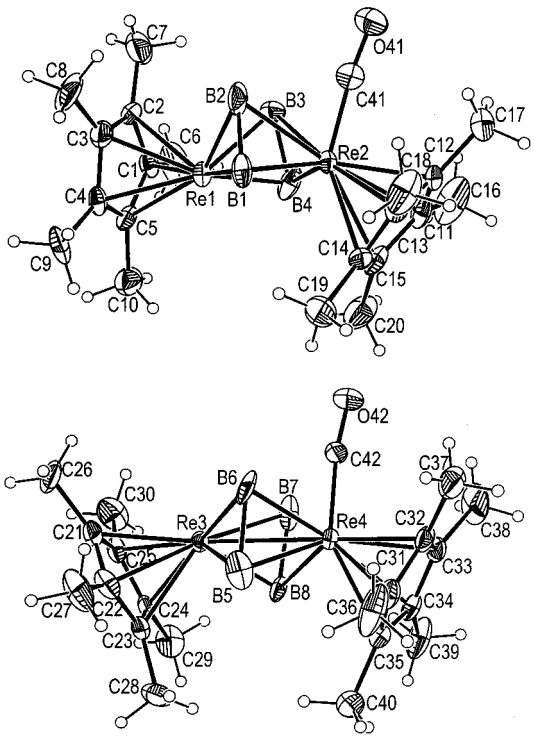

Figure 2. Molecular structures of $(Cp^*ReH_2)(Cp^*ReCO)(B_2H_3)_2$ (**4**) (two independent molecules shown): top, **4**-*trans*; bottom, **4**-*cis*.

Isolation of a Precursor to $(Cp^*ReH_2)(Cp^*ReCO)B_4H_4$ (3). The room-temperature reaction of **2** with CO at 1 atm produces a single metallaborane product, $(Cp^*ReH_2)(Cp^*ReCO)(B_2H_3)_2$ (**4**), in a matter of minutes. On heating, **3** is formed as the sole product; hence, **4** is the precursor to **3**. Before the solid-state structure was obtained, we were unable to satisfactorily explain the spectroscopic data for this metastable intermediate. Hence, the molecular structure in the solid state (Figure 2; Tables 1 and 3) is discussed first. The solution to the spectroscopic puzzle became apparent when the two independent molecules of **4** found in the crystallographic asymmetric unit were discovered to have different geometries, albeit the same connectivities. There are several precedents for such an observation in organometallic chemistry, e.g., $[Cp^*RuCl_2]_2$[43] and $Cp_2W_2Os(CO)_7(CC_6H_4Me)_2$.[44]

In terms of structure, consider the ancillary ligands first. In one of the isomers of **4** (top of Figure 2, designated **4**-*trans*), the Cp* ligands are arranged in a transoid fashion (Re—Re—Cp*(c) = 167, 134°; Cp*(c) = centroid of Cp* ring), as found in **3** (Figure 1). In the other isomer, the Cp* ligands are oriented in a cisoid arrangement, as found in **2**, and hence, it is designated as **4**-*cis* (Re—Re—Cp*(c) = 149, 154°). This implies that the rhenium hydrides and CO ligand are transoid in **4**-*trans* and cisoid in **4**-*cis*. Again the hydrogen atoms were not located in **4**, and positioning of the remainder of the hydrogen atoms rests on the NMR data discussed below.

The second qualitative difference between the structures of **4** and **3** lies in the connectivities of the boron fragments. In **3**,

(42) Weller, A. S.; Shang, M.; Fehlner, T. P. *Organometallics* **1999**, *18*, 853.

(43) Kölle, U.; Kossakowski, J.; Klaff, N.; Wesemann, L.; Englert, U.; Heberich, G. E. *Angew. Chem., Int. Ed. Engl.* **1991**, *30*, 690.

(44) Shapley, J. R.; Park, J. T.; Churchill, M. R.; Bueno, C.; Wasserman, H. J. *J. Am. Chem. Soc.* **1981**, *103*, 7385.

Chart 2

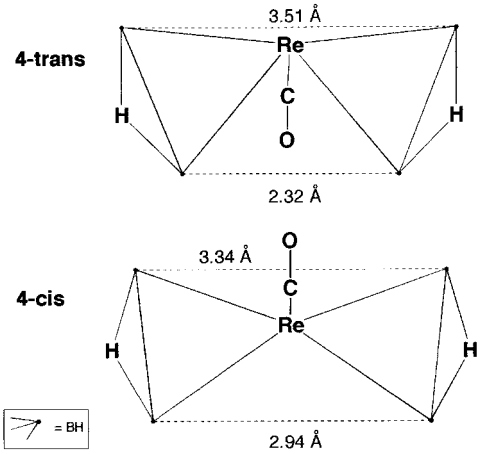

there is a single, planar, open B_4 fragment whereas, in **4**, there are two distinct B_2 fragments; i.e., in going from **4** to **3**, the two B_2 fragments move together and a B−B bonding interaction is formed, fully consistent with the loss of two cluster bonding electrons as H_2. Another difference between the core structures of **4**-*trans* and **4**-*cis* is the placements of the B_2 fragments around the Re−Re bond axes. This is illustrated in Chart 2, where the two Re_2B_2 tetrahedra are viewed down each Re−Re bond. In **4**-*trans*, the difference of the two nonbonded B−B distances between the tetrahedra is larger than that in **4**-*cis*. The CO ligand bisects the shorter distance in **4**-*trans* as with **3** (this places the Re hydrides on the more open side as with **2** and **3**) whereas the CO ligand bisects the longer distance in **4**-*cis*, which also places the Re hydrides on the more open side. Presumably, preferential positioning the two Re hydrides in the more open face is due to the fact that two hydrogens require more space than one CO. There are distinct differences in the Re−Re distances, as well (2.7730(7) Å in **4**-*trans* and 2.8274(7) Å in **4**-*cis*). Finally, all the B−B and Re−B distances are reasonable for a metallaborane of this type.

The spectroscopic data for the mixture of the two isomers in solution provide more detail. On the basis of relative intensities, the isomeric forms have a nearly 1:1 ratio in solution, and cooling results in no significant change in the ^{1}H NMR spectrum. Mild heating simply converts **4** into **3**. This implies either equal stabilities or a significant rearrangement barrier. Both explanations are possible; however, we favor the latter. This would imply kinetic control of the CO addition with equal probability of attack from the two distinct sides of **2** (Scheme 4).

There are two distinct terminal carbonyl stretches in the IR spectrum. Because both **3** (CO band at 1926 cm^{-1}) and **4**-*trans* have transoid geometries and similar Re−Re distances, the band at 1923 cm^{-1} has been assigned to **4**-*trans* and that at 1889 cm^{-1} to **4**-*cis*. The presence of two types of carbonyls is confirmed by the ^{13}C NMR spectrum. However, although the four skeletal boron resonances in the ^{11}B NMR spectrum, the four methyl resonances plus four BH (terminal) resonances in the ^{1}H NMR spectrum, and the four Cp* resonances in the ^{13}C NMR spectrum are consistent with the presence of two isomers, specific assignments are not possible. In the high-field region of the ^{1}H NMR spectrum of **4**, the resonances at δ −2.0 (4 H) and −12.6 (2 H) show coupling to boron whereas that at δ −14.4 (2 H) shows little coupling (according to ^{1}H{selective ^{11}B} NMR spectroscopy). The signature of the δ −14.4 resonance is much like that of **3**, and it is assigned to the **4**-*trans* isomer; i.e., its cage structure is more similar to that of **3** than is that of **4**-*cis*. By difference, the δ −12.6 resonance is assigned to **4**-*cis*, and consistent with its geometry, stronger interactions of the Re hydrides with the adjacent boron atoms are implied by larger couplings to the borons. The resonance at δ −2.01 has been assigned to accidental overlap of the two pairs of B−H−B hydrogens on **4**-*trans* and **4**-*cis*, which are, in fact, in similar environments. These assignments are summarized in the representations of the structures of the two isomers given in Scheme 4.

Comparison of the Reactions of $(Cp^*ReH_2)_2B_4H_4$ and $(Cp^*Cr)_2B_4H_8$ with CO. At the level of electron counting, the reactions are similar—6-sep **2** gives 6-sep **3** whereas 5-sep $(Cp^*Cr)_2B_4H_8$ gives 6-sep $(Cp^*CrCO)_2B_4H_6$. In both cases, an electronically saturated molecule is the end product. In addition to the compositional and structural differences between **3** and$(Cp^*CrCO)_2B_4H_6$, there is a large difference in the rates of the two processes. Addition of CO to **2** to give **4** occurs in minutes at room temperature whereas the same reaction for $(Cp^*Cr)_2B_4H_8$ requires days at room temperature. Second, although addition of CO to **2** is facile, loss of H_2 to convert **4** to **3** is slow at room temperature. If $\{(Cp^*CrCO)_2B_4H_8\}$ is an intermediate in the formation of $(Cp^*CrCO)_2B_4H_6$, the barrier for H_2 loss must be smaller than that for CO addition because no intermediate was observed by NMR spectroscopy.[10] It is possible that CO addition is facilitated by the larger Re metal center compared to Cr and that the H_2 elimination barriers are about the same. Whatever the ultimate cause of these differences, certainly they can be attributed to the roles played by the transition metals in the reactions.

Reaction of $(Cp^*ReH_2)_2B_4H_4$ with $Co_2(CO)_8$. The reactions of transition metal fragment sources with metal clusters generally result in metal fragment substitutions or additions.[45] Although less well studied, the same is true of such reactions involving metallaboranes.[46,47] Hence, we have investigated the reaction of $Co_2(CO)_8$ with **2**. The net result is the addition of two cobalt fragments to give 6-sep $(Cp^*Re)_2B_4H_4Co_2(CO)_5$ (**5**) (Scheme 5).

The mass and ^{1}H NMR spectra of **5** show the loss of the 4 Re−H hydrogens of **2**. The ^{11}B and ^{1}H NMR spectra suggest the presence of two planes of symmetry and retention of the relative rhenium and boron atom geometries found in **2**. The IR spectrum exhibits a carbonyl stretching pattern (terminal and bridging) typical of that observed for compounds containing an $M_2(CO)_n$ fragment, which, in turn, suggests a $Co_2(CO)_5$ fragment closing the open face of **2**. These data do not permit a distinction between an orientation of the Co_2 fragment perpendicular to the plane of the B_4 fragment, like that in $(Cp^*Re)_2B_7H_7$ (Scheme 3), and one parallel to this plane.

The full geometry of **5** is defined by a solid-state structure determination, and the molecular structure is shown in Figure 3. The Re_2B_4 skeleton of **2** is retained, and the open face is closed by a 4-electron $Co_2(CO)_5$ fragment placed coplanar with the B_4 fragment. Effectively, the four endo-hydrogens on the open face of **2** are replaced by the $Co_2(CO)_5$ fragment. With 8 cluster fragments and only 6 skeletal electron pairs, the cluster is hypoelectronic like $(Cp^*Re)_2B_7H_7$. Consistent with the subcloso electron count, the cluster shape is not the structural motif expected for a closed eight-vertex cage, i.e., a dodecahedron.. Not unexpectedly then, the cross-cage Re−Re distance of 2.6393(5) Å falls in the range associated with Re−Re single

(45) *The Chemistry of Metal Cluster Complexes*; Shriver, D. F., Kaesz, H. D., Adams, R. D., Eds.; VCH: New York, 1990.
(46) Lei, X.; Shang, M.; Fehlner, T. P. *Organometallics* **1998**, *17*, 1558.
(47) Lei, X.; Shang, M.; Fehlner, T. P. *Chem. Commun.* **1999**, 933.

Scheme 6

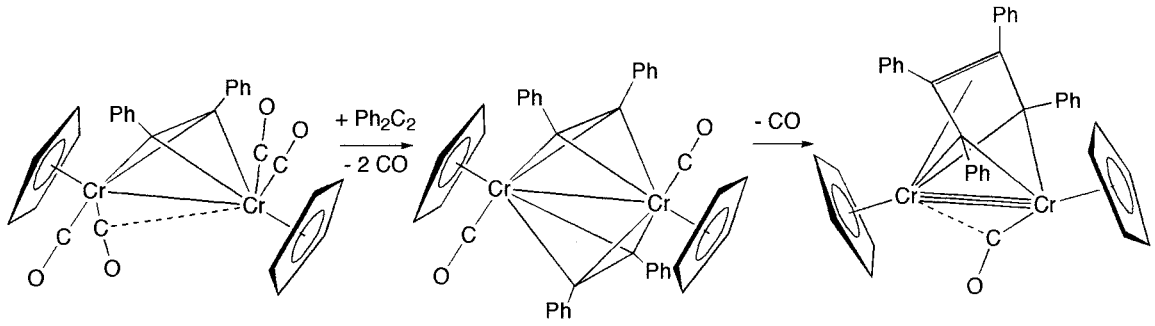

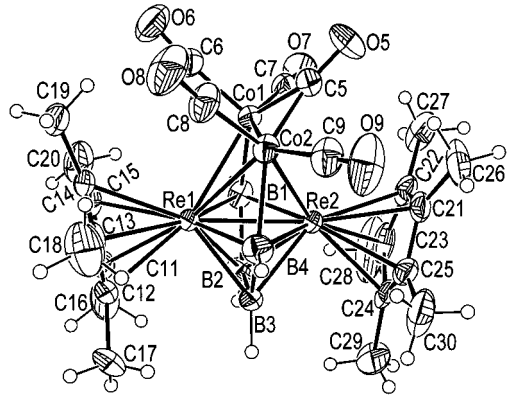

Figure 3. Molecular structure of $(Cp^*Re)_2\{\mu\text{-}\eta^6\text{:}\eta^6\text{-}B_4H_4Co_2(CO)_5\}$ (**5**).

bonds.[24,48] An alternative description of **5** as a 24-valence-electron triple-decker complex, $(Cp^*Re)_2\{\mu\text{-}\eta^6\text{:}\eta^6\text{-}B_4H_4Co_2(CO)_5\}$, has been presented earlier.[19] The rigorous planarity of the closed, six-member $B_4H_4Co_2(CO)_5$ ring makes this description particularly appropriate and permits comparison with the 24-valence-electron triple-decker complex $(CpCr)_2\{\mu\text{-}\eta^6\text{:}\eta^6\text{-}B_4H_4C_2R_2\}$.[49]

As before, the reaction of **2** with a typical metal fragment source is qualitatively different from that observed for $(Cp^*Cr)_2B_4H_8$.[17] As noted in the Introduction, this chromaborane reacts with $Co_2(CO)_8$ to give $(Cp^*Cr)_2B_4H_7Co(CO)_3$, which is viewed as a metal complex of the chromaborane. The compound $(Cp^*Cr)_2B_4H_8Fe(CO)_3$ is even more easily viewed as an adduct.[18] The rhenaborane undergoes a more extensive reaction, but the nature of the product observed in each case suggests a relationship between the reactions.

We previously proposed that, in the reaction of a metallaborane with $Co_2(CO)_8$, a cluster H is replaced with a $Co(CO)_4$ fragment, with concurrent generation of $HCo(CO)_4$.[12,46,47] Thus, the reaction of **2** might be viewed as

$$(Cp^*ReH_2)_2B_4H_4 + Co_2(CO)_8 \rightarrow \{(Cp^*Re)_2H_3B_4H_4Co(CO)_3\} + HCo(CO)_4 + CO$$

$$\{(Cp^*Re)_2H_3B_4H_4Co(CO)_3\} + Co_2(CO)_8 \rightarrow \{(Cp^*Re)_2B_4H_4Co_2(CO)_5\} + HCo(CO)_4 + 2CO + H_2$$

The first intermediate is analogous to $(Cp^*Cr)_2B_4H_7Co(CO)_3$. Thus, once again, the difference in reactivity can be associated with the different natures of the endo-hydrogens in the rhena- and chromaboranes.

Relevance

The reactivities of $(Cp^*M)_2B_4H_8$, M = Cr, Re, with three different test reactants clearly illustrate the importance of the transition metals in determining their properties. Despite the similar geometric structures and identical stoichiometries of these compounds, the reactivity associated with the rhenaborane is more facile and more extensive. On the basis of a comparison of the spectroscopic data, these differences are associated with the endo-hydrogen atoms of the metallaborane cluster. In the chromaborane, these hydrogen atoms are similar to those in boron hydrides whereas, in rhenaborane, they are much more like metal hydrides—properties that are expressed in reactivity.

One of the interesting aspects of metallaborane chemistry is its connection to organometallic chemistry.[50] An example from the present chemistry reinforces this connection. In a discussion of the linking of alkynes at group 6 dimetal centers, Knox et al. favor the route shown in Scheme 6 for one of the systems studied.[51] Comparison with Scheme 4 easily shows that the conversion of **4** to **3** is pleasingly similar to the postulated final step in the organometallic system—loss of H_2 results in B−B bond formation just as loss of a CO ligand results in C−C bond formation. A related B−B coupling reaction concurrent with H_2 elimination has been observed in a more hydrogen-rich system, i.e., the conversion of $(Cp^*IrH)_2(B_2H_4)_2$ to $(Cp^*Ir)_2B_4H_8$.[13] Thus, the manipulation of boranes with transition metals provides an informative counterpoint to the chemistry of hydrocarbyls with metals.

Acknowledgment. We thank Dr. Christopher L. Cahill for assistance with the X-ray crystallography and Mr. Donald Schifferl for skillful technical assistance with the NMR experiments. The generous support of the National Science Foundation is gratefully acknowledged.

Supporting Information Available: Crystallographic data, CIF files, for **3**−**5**, deposited with refs 19 and 20. Please refer to these references for retrieval instructions.

IC0006091

(48) Poli, R.; Wilkinson, G.; Moetevailli, M.; Hursthouse, M. B. *J. Chem. Soc., Dalton Trans.* **1985**, 931.
(49) Kawamura, K.; Shang, M.; Wiest, O.; Fehlner, T. P. *Inorg. Chem.* **1998**, *37*, 608.
(50) Fehlner, T. P. In *The Synergy Between Dynamics and Reactivity at Clusters and Surfaces*; Farrugia, L. J., Ed.; NATO ASI Series, C; Kluwer Academic Publishers: Dordrecht, The Netherlands, 1995; Vol. 465; p 75.
(51) Knox, S. A. R.; Stansfield, R. F. D.; Stone, F. G. A.; Winter, M. J.; Woodward, P. *J. Chem. Soc., Dalton Trans.* **1982**, 173.